이학석사 학위논문

CD56+CD57+ natural killer cell infiltration is associated with antibody-mediated rejection in kidney transplantation

신장 이식 후 항체-매개성 거부반응과 CD56+CD57+ 자연살상세포 침윤과의 연관성 규명 연구

울 산 대 학 교 대 학 원

의 과 학 과

정 혜 림

CD56+CD57+ natural killer cell infiltration is associated with antibody-mediated rejection in kidney transplantation

지 도 교 수　신　성

이 논문을 이학석사 학위 논문으로 제출함

2020년 02월

울 산 대 학 교 대 학 원

의 과 학 과

정 혜 림

정혜림의 이학 석사학위 논문을 인준함

심사위원 김 헌 식 (인)

심사위원 이 종 원 (인)

심사위원 신 성 (인)

울 산 대 학 교 대 학 원

2020 년 02 월

Abstract

Natural killer (NK) cells have crucial functions in antibody-mediated rejection (ABMR) and graft failure after kidney transplantation. However, the features and clinical indications of specific subsets of infiltrated NK cells have not been fully evaluated yet. Thirty-nine clinically indicated transplant biopsies performed at Asan Medical Center from May 2015 to July 2017 were analyzed by Opal multiplex immunohistochemistry (IHC). Study groups were classified into three different groups as no rejection (NR) group, T cell-mediated rejection (TCMR) group, and antibody-mediated rejection (ABMR) group according to histopathologic reports; 8 patients (20.5%) belonged to the NR group, 11 (28.2%) to the TCMR group, and 20 (51.3%) to the ABMR group. Paraffin-embedded sections of 39 renal biopsies were labeled using Opal™ multiplex kit (PerkinElmer®). Anti-CD3, anti-CD56, anti-CD57, anti-CD49b, anti-NKG2A, and anti-KIR antibodies were used to define NK cells. NK cells were defined as $CD3^{-}CD56^{+}$ lymphocytes that are positive for CD57, CD49b, NKG2A, or KIR. Opal™ multiplex IHC revealed that the density of NK cells was significantly higher in the ABMR group (2.57 ± 2.58/mm2) than in the NR (0.12 ± 0.22 /mm2) or the TCMR (0.25 ± 0.34/mm2) group (P = .002). Remarkably, infiltrated CD3-CD56+CD57+ cells (2.16 ± 1.89) were the most frequently detected compared with CD3-CD56+CD49b+ (0.05 ± 0.13), CD3-CD56+NKG2A+ (0.21 ± 0.69), and CD3-CD56+KIR+ (0.15 ± 0.42) cells in the ABMR group (P < .001). Kaplan-Meier survival analysis revealed that death-censored graft failure was significantly higher in recipients with NK cells infiltration compared to those without NK cells infiltration (Log-rank test, p=0.025). In conclusion, infiltrated CD56+CD57+ cells are the main subset of NK cells in kidney transplant recipients with ABMR, and the presence of infiltrated NK cells is associated with graft failure post-transplant.

Table of Contents

List of Tables

List of Figures

List of Abbreviations

NK, natural killer

ABMR, antibody-mediated rejection

NR, no rejections

TCMR, T cell-mediated rejections

DSA, donor-specific antibody

PAS, periodic acid-Schiff

H&E, hematoxylin and eosin

IFTA, interstitial fibrosis and tubular atrophy

FFPE, formalin-fixed paraffin-embedded

MWT, microwave treatment

ROI, region of interest

PBMC, peripheral blood mononuclear cell

DCGF, death-censored graft failure

SD, standard deviation

AUC, area under the receiver operating characteristics curve

AHR, adjusted hazard ratio

ADCC, antibody-dependent cell-mediated cytotoxicity

KIR, killer immunoglobulin-like receptor

CMV, human cytomegalovirus

Introduction

Kidney transplantation is the therapy of choice available for most patients with end-stage kidney disease (ESRD). After solid organ transplantation, the leading cause of late allograft failure is antibody-mediated rejection (ABMR), and it also contributes to two-thirds of kidney transplant[1,2]. Recently, donor-specific antibodies (DSAs) were reported as an important prognostic factor for kidney allograft survival[3,4]. In recent years, kidney allograft survival has significantly increased with the development of potent immunosuppression regimens; however, most of the current immunosuppressants commonly target T cells to prevent T cell-mediated rejection (TCMR). Because of the important role of DSAs in ABMR, several therapies with depleting B cells and DSAs have been developed with inactivation of plasma cells, although most of these therapies have limitations to prevent and to treat ABMR[5-7]. Thus, novel approaches are necessary for studying and developing to prevent and to treat ABMR with improving clinical outcomes after kidney transplantation. Therefore, novel strategies that prevent and treat ABMR need to be developed in order to further improve clinical outcomes after kidney transplantation.

NK cells are paradoxically associated with both graft acceptance and dysfunction through their influence on relevant immune pathways[8-10]. Recent studies utilized microarray transcriptomic data to determine that NK cells perform a central role in the pathophysiology of ABMR and graft failure after kidney transplantation[11-13]. However, the exact mechanism of NK cells and markers of NK activation for ABMR are not still determined. While first evaluated as an NK cell marker, CD57 has been almost considered as a marker of replicative senescence on T cell[14]. According to a recent report, acquisition of CD57 reflects a higher cytotoxic capacity, greater responsiveness to signaling, and reduced responsiveness to cytokines rather than being a marker of immunosenescence or anergy[15,16]. Also, NK cells were demonstrated as important effector during the host innate immune response to viral infection as a human cytomegalovirus (CMV), which is a member of the Herpesviridae family. CMV

drives expansion of NKG2C+ NK cells and that these cells preferentially acquire CD57[17,18]. On the other hand, NK cells, which interact with HLA-E and distinct sets of classical HLA class I molecules, are inactivated by the killer immunoglobulin-like receptor (KIR) family and CD94/NKG2A heterodimer[19-21].

So far, it has been unrevealed which subsets of NK cells are associated with ABMR after kidney transplantation. In this study, he specific subsets of infiltrated NK cells in human kidney transplant biopsies would be characterized by using multiplex immunohistochemistry and investigated clinical implications of each NK cell subset concerning graft survival.

Material and Methods

Patients

Thirty-nine for-cause kidney transplant biopsies, performed at Asan Medical Center between May 2015 and December 2016, were analyzed in this study. Kidney transplant recipients, who had a clinical indication such as proteinuria or deterioration in function in five years after kidney transplantation, were enrolled by consent. The recipients, who had a pediatric kidney transplant or multiple solid organ transplants, were excluded in this study. All enrolled recipients consented written informed consent. The institutional review board (IRB) of Asan Medical Center approved this study with approval number: 2015-0758. After receiving approval from IRB, baseline characteristics and all clinical data were recorded and evaluated.

Organ or tissues were not obtained from prisoners. There were not possible to get informed consent from a kidney donor at the time of a for-cause biopsy. The lack of informed consent of kidney donors was approved by the same IRB of this study. A government organization (KONOS, Korean Network for Organ Sharing) strictly managed every deceased donor without any organ trade or illegal distribution.

All experiments were followed by accordance with relevant guidelines and regulations.

Immunosuppression

As an induction regiment, rabbit anti-thymocyte globulin (Thymoglobulin®, Genzyme, Cambridge, MA, USA) was treated in three patients, and basiliximab was treated in thirty-six patients. A mycophenolic acid, calcineurin inhibitor (tacrolimus or cyclosporine), and prednisolone were components of the maintenance immunosuppressants.

Histopathology

All biopsies of recipients included at least seven glomeruli and one artery for classification and diagnosis of rejection. Hematoxylin and eosin (H&E), Periodic acid-Schiff (PAS), Jones-methenamine silver, and Masson trichrome were progressed on each biopsy to

interpret and analyze rejection. C4d immunohistochemistry (1:100, rabbit polyclonal; Cell Marque, Rocklin, CA, USA) was proceeded formalin-fixed paragon-embedded tissue specimen by using the Ventana Medical Systems(Tucson, AZ, USA) according to the manufacturer's protocol[22]. According to the Banff 2015 criteria[23], every transplant biopsy specimen was appraised for histologic characteristics by two renal pathologist (YM Cho and H Go in Department of Pathology, Asan Medical Center, University of Ulsan College of Medicine, Seoul, Korea), and biopsies without histological disease characteristics were diagnosed as normal. C4d staining ≥ 10% was classified as positive. Interstitial fibrosis and tubular atrophy (IFTA) was defined with more than 0 on ci score. Also, two pathologists (YM Cho and H Go) scored Inflammation in IFTA areas (i-IFTA) according to the Banff 2017 criteria[24].

Opal multiplex immunohistochemistry

Method of Opal multiplex immunohistochemistry with seven-color staining was fully automated by using Leica Bond Rx™ Automated Stainer (Leica Biosystems) with Opal™ multiplex kit (PerkinElmer®) in the Optical Imaging Core Laboratory at Asan Institute for Life Sciences, Asan Medical Center.

Before progress the Leica Bond Rx™ Automated Stainer, the FFPF tissue block slides were heated at 60 ℃ for four hours in a dry oven. Through the Leica Bond Rx™ Automated Stainer, deparaffinization was firstly performed by rinsing the slides with 100% xylene for ten minutes, repeated three times. In citrate buffer with pH 6.0, antigen retrieval was conducted by using microwave treatment (MWT). After antigen retrieval, the sample slides were rinsed and blocked with 3% H_2O_2 blocking solution, and then the antibodies were diluted. The six different primary antibodies – KIR (LSBio, rabbit polyclonal, dilution 1:200), CD3 (Dako, rabbit polyclonal, dilution 1:100), CD56 (Leica Biosystem, mouse monoclonal, clone CD564, dilution 1:100), NKG2A (Abcam, rabbit polyclonal, dilution 1:100), CD57 (Thermofisher, mouse monoclonal, clone NK1, dilution 1:100), and CD49b (GeneTex, mouse monoclonal, clone 16B4, dilution 1:50) – were respectively incubated for one hour each staining step with

optimized concentrations, followed by Opal HPR Ms+Rb kit and Opal fluorophores (KIR: Opal 520, CD3: Opal 540, CD56: Opal 570, NKG2A: Opal 620, CD57: Opal 650, CD49b: Opal 690) were used to visualize antigens.

Afterward, stripping of antibody complexes was individually performed after each round of antigen detection with Opal HPR Ms+Rb kit and Opal fluorophores. From blocking step to antibody stripping step were repeated until all antibodies were stained and until all antigens were visualized by using different Opal fluorophores for each target. The last step, after the final stripping step, was performed to stain nuclei with DAPI included in the Opal™ multiplex kit (PerkinElmer®), and cover-slipped by using HIGHDEF® IHC fluoromount (ADI-950-260-0025, Enzo, USA)[25,26].

Image acquisition and quantitative image analysis

Through Vectra® Polaris Automated Quantitative Pathology Imaging System (PerkinElmer®), multiplex-stained biopsy slides were scanned, and all target cell markers on the slides were visualized as multispectral images. Region of Interest (ROI) Tool in Phenochart software was used to designate ROIs on each scanned biopsy slide as many as possible to analyze most of the whole biopsy tissue; therefore, biopsy slides had different number of ROIs. The spectral information was collected as raw data reliably and quantitated

For quantification of the spectral information without mixed, a multispectral library should be established including exact examples of each fluorophore emission spectra in addition to a representative autofluorescence spectrum[25]. Consequently, the library for multispectral analysis was confirmed by individually stained sections (KIR: Opal 520, CD3: Opal 540, CD56: Opal 570, NKG2A: Opal 620, CD57: Opal 650, CD49b: Opal 690). After all biopsy slides were visualized as images, the spectral composite images were created by an analysis algorithm in InForm 2.4 software, and the exported data and images were analyzed through Spotfire software (TIBCO Software Inc.). Each cell on biopsy tissue was identified by fluorescent stain with DAPI. The cells that were detected $CD3^{-}CD56^{+}$ overlapped with at least one of the NK subsets (CD57, CD49b, NKG2A, and KIR)-positive were identified as

infiltrated NK cells. Infiltrated $CD3^+CD56^-$ cells were considered as T cell whereas $CD3^+CD56^+$ as NKT cells. Raw counts of infiltrated NK cells, T cells, and NKT cells were counted by using Spotfire software (TIBCO Software Inc.), and densities of NK cells and T cells on each biopsy slide was calculated that raw count of NK cells and T cells divided by total area of ROIs, which was calculated by total number of ROIs in each slide multiplied by 0.69 mm2 (one ROI: 1 field = 0.69 mm^2, 1 field = 2,628,288 pixels, 1 pixel = 0.5112 μm × 0.5112 μm). If infiltrated cells were positive for more than three out of four NK markers (CD57, CD49b, NKG2A, and KIR), they were repeatedly counted and divided by the number of positive markers to belong to each subpopulation of infiltrated NK cells.

HLA antibody testing and HLA typing

Previous study at our center had been described HLA antibody testing and HLA typing[27]. LABScreen® Single Antigen Class I and Class II assay (One Lambda Inc., Canoga Park, CA) was used to determine antibody specificities. Antibodies against HLA-A, -B, -C, -DRB1, -DRB3, -4 and -5, and -DQB1 were examined by using single antigen beads. Low-to-medium resolution HLA-A, -B, -C and DR typing was performed using BioSewoom™ PCR/SSP kit (BioSewoom Inc., Seoul, Korea) and high resolution HLA-DQB1 typing was done by AVITA™ plus HLA-DQB1 SBT kits (BioWithus Inc., Seoul, Korea).

Clinical outcomes

The primary clinical outcome was death-censored graft failure (DCGF).

Statistical analysis

The presentation of categorical variables was represented as absolute and relative frequencies. The presentation of quantitative variables was represented as mean and standard deviation (SD). Student's t-test or Mann-Whitney U test was used to analyze differences between means, as appropriate. Densities of infiltrated NK cells according to histologic diagnosis were compared by one-way analysis of variance. The chi-squared test was used to compare categorical variables. To evaluate the ability of infiltrated NK cells to differentiate

histologic ABMR from other study groups, the area under the receiver operating characteristics curve (AUC) was calculated. Cox proportional hazard model was used for univariate and multivariate analyses. Death-censored graft survival rate was calculated using the Kaplan-Meier method and compared using the log-rank test. A test for the proportionality property of hazards was performed for each factor considered within the multivariate model. P values < 0.05 were considered statistically significant. All statistical analyses were performed using SPSS version 21.0 for Windows (SPSS Inc., Chicago, IL, USA).

Results

Patient characteristics and histopathology

Thirty-nine kidney transplant recipients were enrolled to collect indication biopsies, and their indication biopsies were analyzed through Opal multiplex immunohistochemistry (IHC) in this study. Clinical and demographical characteristics were shown in Table 1. The study groups were classified into no rejection (NR; n = 8) group, T cell-mediated rejection (TCMR; n = 11) group, and antibody-mediated rejection (ABMR; n = 20) group (Table 1). Out of the 20 patients in the ABMR group, nine patients had a mixed rejection (TCMR + ABMR). The Mean interval between kidney transplantation and for-cause biopsy was 23.1 ± 16.3 months. The ABMR group had a longer time to the biopsy after kidney transplantation compared with the NR group (27.4 ± 16.7 vs. 10.5 ± 14.4 months, $P = .03$). There was no significant difference in terms of baseline characteristics between groups otherwise. In the TCMR group, borderline rejection was diagnosed in 8 (72.7%) specimens; type IA rejection was diagnosed in 2 (18.2%) specimens; type IB rejection was diagnosed in 1 (9.1%) specimens. Among the 9 patients who had mixed rejection, type IA TCMR was in 4 (44.4%) and type IB TCMR in 5 (55.6%) specimens. In ABMR group, 14 of 20 patients had acute active ABMR (70%), and 6 of 20 patients had chronic active ABMR (30%). IFTA was diagnosed in 32 specimens (82.0%), which were equally divided between mild and moderate-to-severe IFTA (Table 2). Based on the mean of Banff scores, the AMBR group had significantly higher mean scores of i score (Interstitial Inflammation), ci score (Interstitial Fibrosis), and ti score (Total Inflammation) than NR group. The ABMR group had significantly higher mean scores of g score (Glomerulitis) than TCMR group, and it also had a higher mean of ptc score compared with the TCMR group.

Table 1. Clinical and demographic characteristics of patients with for-cause biopsy.

Variables	Total (n = 39)	NR (n = 8)	TCMR (n = 11)	ABMR (n = 20)	*P-value*
Mean age, y (SD)	43.7 (12.8)	45.5 (15.4)	46.0 (9.8)	42.6 (13.3)	0.735
Female sex, n (%)	8 (20.5)	2 (25.0)	1 (1.9)	5 (25.0)	0.789
Body mass index, kg/m2 (SD)	22.4 (2.7)	21.5 (3.7)	21.6 (2.7)	22.8 (2.4)	0.475
Deceased donor, n (%)	13 (33.3)	3 (37.5)	3 (27.3)	7 (35.0)	0.806
Previous transplant, n (%)	9 (23.1)	3 (37.5)	1 (1.9)	5 (25.0)	0.715
Time to biopsy, month (SD)	23.1 (16.3)	10.5 (14.4)	24.3 (12.9)	27.4 (16.7)	0.03
Cause of ESRD, n (%)					0.187
Glomerular	5 (12.8)	2 (25.0)	0	3 (15.0)	
Diabetes	6 (15.4)	1 (12.5)	3 (27.3)	2 (10.0)	
Hypertension	4 (10.3)	2 (25.0)	0	2 (10.0)	
FSGS	1 (2.6)	1 (12.5)	0	0	
Other	17 (43.6)	2 (25.0)	6 (54.4)	9 (45.0)	
Unknown	6 (15.4)	0	2 (18.2)	4 (20.0)	
ABO-incompatible KT	10 (25.6)	3 (37.5)	3 (27.3)	4 (30.0)	0.625

Serum creatinine at the time of biopsy, mg/dL (SD)	2.7 (1.9)	2.7 (2.5)	2.3 (0.8)	2.9 (2.1)	0.746
PRA > 10%, n (%)	18 (46.2)	5 (62.5)	2 (18.2)	11 (55.0)	0.853
DSA at the time of biopsy, n (%)	22 (56.4)	4 (50.0)	3 (27.3)	15 (75.0)	0.088
CNI at the time of biopsy, n (%)					0.789
Cyclosporine	8 (20.5)	0	5 (45.5)	3 (15.0)	
Tacrolimus	31 (79.5)	8 (100)	6 (45.)	17 (85.0)	
Follow-up after biopsy, month (SD)	46.7 (19.1)	38.1 (20.7)	49.1 (14.5)	48.8 (20.5)	0.317

NR, no rejection; TCMR, T-cell-mediated rejection; ABMR, antibody-mediated rejection SD, standard deviation; ESRD, end-stage renal disease; FSGS, focal segmental glomerulosclerosis; KT, kidney transplantation; PRA, panel-reactive antibody; DSA, donor specific antibody; CNI, calcineurin inhibitor

Table 2. Comparison of histopathologic characteristics according to histologic diagnosis

Variables	Total (n = 39)	NR (n = 8)	TCMR (n = 11)	ABMR (n = 20)	*P-value*
Histopathology, n (%)					0.009
TCMR only	11 (28.2)	0	11 (100)	0	
ABMR only	11 (28.2)	0	0	11 (55.5)	
ABMR + TCMR	9 (23.1)	0	0	9 (45.5)	
No rejection	8 (20.5)	8 (100)	0	0	
C4d staining, n (%)					0.747
< 10%	34 (87.2)	7 (87.5)	9 (81.8)	18 (90.0)	
≥ 10%, < 50%	5 (12.8)	1 (12.5)	2 (18.2)	2 (10.0)	
≥ 50%	0	0	0	0	
IFTA, n (%)					0.02
Minimal	7 (17.9)	4 (50.0)	1 (9.1)	2 (10.0)	
Mild	16 (41.0)	2 (25.0)	7 (63.6)	7 (35.0)	
Moderate-to-severe	16 (41.0)	2 (25.0)	3 (27.3)	11 (55.0)	
Mean Banff score, mean (SD)					
g	0.79 (0.83)	0.75 (1.04)	0.27 (0.47)	1.1 (0.79)	0.025
cg	0.31 (0.73)	0.13 (0.35)	0.09 (0.3)	0.5 (0.95)	0.246
mm	0.15 (0.37)	0.25 (0.46)	0.18 (0.41)	0.1 (0.31)	0.603
i	1.49 (1.07)	0.5 (0.76)	1.27 (0.91)	2.00 (0.97)	0.001
ci	1.26 (0.97)	0.5 (0.76)	1.18 (0.75)	1.6 (0.99)	0.019
t	1.46 (1.02)	0.75 (1.17)	1.64 (0.81)	1.65 (0.99)	0.084
ct	1.33 (1.18)	0.63 (0.74)	1.27 (0.65)	1.65 (0.93)	0.019
v	0.05 (0.22)	0.13 (0.35)	0	0.05 (0.22)	0.496
cv	1.05 (1.03)	0.63 (0.74)	1.27 (1.27)	1.1 (0.97)	0.389

ah	0.82 (102)	0.25 (0.46)	1.36 (1.21)	0.75 (0.97)	0.054
ptc	1.33 (0.97)	0.5 (1.07)	0.45 (1.04)	2.15 (0.59)	< 0.001
ti	1.9 (0.97)	0.88 (0.64)	1.73 (0.65)	2.4 (0.88)	< 0.001
i-IFTA	1.97 (0.99)	1.38 (1.30)	2.22 (0.97)	2.10 (0.79)	0.146

NR, no rejection; TCMR, T-cell-mediated rejection; ABMR, antibody-mediated rejection; IFTA, interstitial fibrosis and tubular atrophy; SD, standard deviation

Variation in the density of infiltration NK cells depending on histologic diagnosis of kidney transplant

The subpopulation was characterized by multiplex immunohistochemistry with six markers (CD3, CD56, CD57, CD49b, NKG2A, and KIR). Infiltrated NK cells were detected in peritubular capillaries and interstitial spaces (Figure 1), and infiltrated NK cells had a lower density than filtrated CD3+ mononuclear cells. Infiltrated NK cells in kidney allografts were stained by multiplex immunohistochemistry, and Figure 1 represents an example of kidney allografts with antibody-mediated rejection and T cell-mediated rejection that is included in ABMR group. Based on the histologic diagnosis, densities of infiltrated CD3+CD56- cells with detected other makers of NK subsets and CD3-CD56+, T cells, were compared by using one-way analysis of variance. The ABMR group ($2.57 \pm 2.58/mm^2$) had significantly higher density of infiltrated NK cells compared to the NR ($0.12 \pm 0.22/mm^2$) and the TCMR ($0.25 \pm 0.34/mm^2$) groups ($P = 0.002$) (Figure 2A). Additionally, the density of infiltrated T cells was significantly higher in the ABMR group ($393.40 \pm 300.93/mm^2$) compared with the NR ($129.83 \pm 119.09/mm^2$) (Figure 2B). The density of NK infiltration is likely correlated with that of T cells only in the ABMR group with marginal significance ($r = .4000$, $P = 0.081$). In the correlation between the density of NK cells and the phenotypes of for-cause biopsy, the density of infiltrated NK cells effectively differentiated ABMR from the TCMR (AUC = 0.95, $P < .001$) and the NR (AUC = 0.92, $P < .001$) groups with good discriminative performance (Figure 3). The subpopulations of infiltrated NK cells were evaluated by histologic diagnosis; consequently, CD3-CD56+CD57+ infiltrated cells were the most predominate subpopulation of infiltrated NK cells in the ABMR group (Figure 4). When one-way analysis of variance was performed to compare the density of $CD56^+CD57^+$ cells between three histologic groups, the density was significantly higher in the ABMR group compared with the NR ($p = .003$) and the TCMR ($p = .002$).

In the ABMR group, moreover, $CD56^+CD57^+$ infiltrates ($2.16 \pm 1.89/mm^2$) were the major subpopulation of NK cells compared with $CD56^+CD49b^+$ ($0.05 \pm 0.13/mm^2$),

$CD56^+NKG2A^+$ (0.21 ± 0.69/mm^2), and $CD56^+KIR^+$ (0.15 ± 0.42/mm^2) cells in the ABMR group (P < .001) when paired t-test was performed. Remarkably, the infiltrated $CD56^+NKG2A^+$ cells were observed only in the ABMR group, although the density (0.21 ± 0.69/mm^2) is low. Meanwhile, $CD56^+CD49b^+$ and $CD56^+KIR^+$ cells were infiltrated mostly in the ABMR group even though there was no statistical significance.

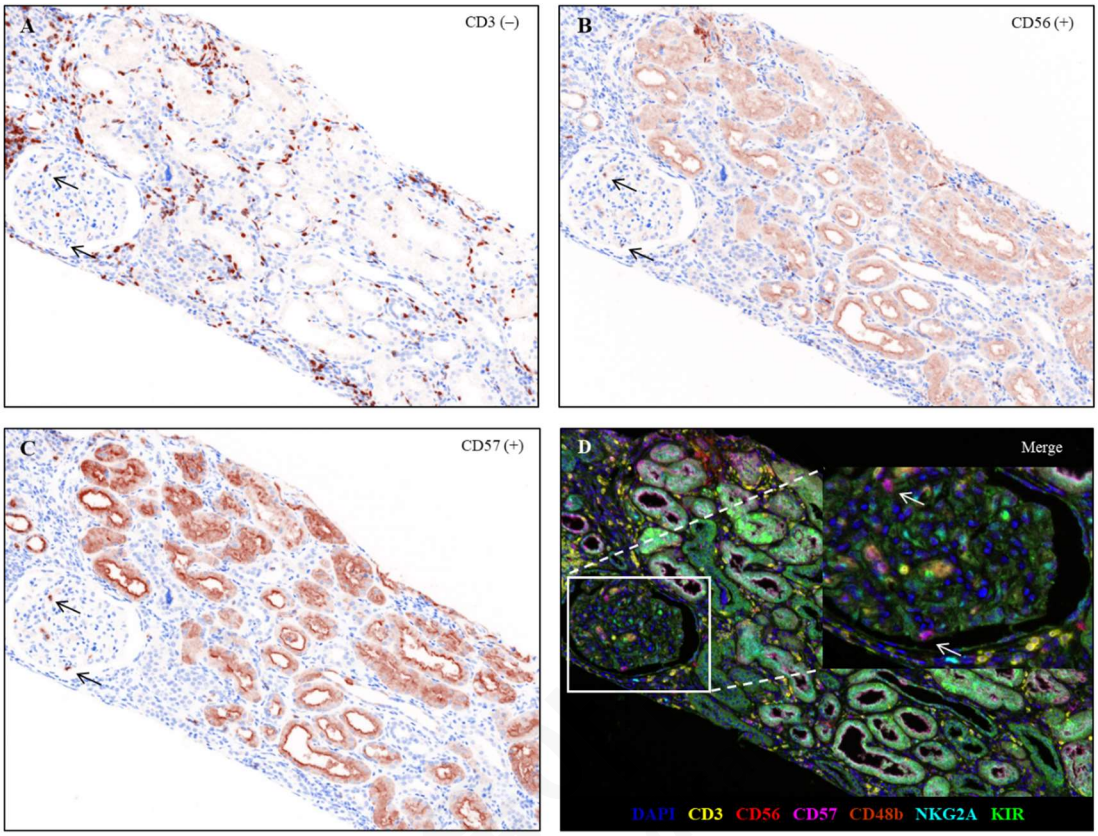

Figure 1. Representative multiplex immunohistochemistry of a kidney allograft with T cell -mediated rejection and antibody-mediated rejection.

Kidney allograft slides were stained with KIR (1:200), CD3 (1:100), CD56 (1:100), NKG2A (1:100), CD57 (1:100), and CD49b (1:50). Black arrows indicate CD3¬ (A), CD56+ (B), CD57+ (C) lymphocytes in the glomerulus. A composite image (D) was created according to spectral library for each Opal fluorophores (KIR: Opal 520, CD3: Opal 540, CD56: Opal 570, NKG2A: Opal 620, CD57: Opal 650, CD49b: Opal 690), and cell phenotypes of infiltrated lymphocytes was designated different colors (DAPI, Blue; KIR, Green; CD3, Yellow; CD56, Red; NKG2A, Cyan; CD57, Magenta; CD49b, Brown)

Inset: higher-magnification view of a section demonstrating CD56+CD57+ NK cells in the glomerulus. Original magnification: x200

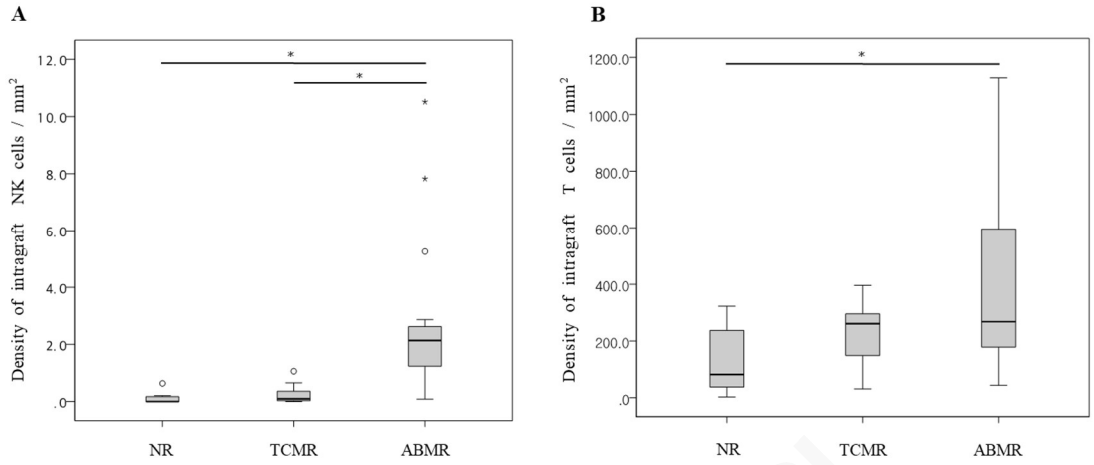

Figure 2. Density of infiltrated NK (A) and T (B) cells according to histologic diagnosis.

(A) The density of the ABMR group was 2.57 ± 2.58/mm^2, the density of the NR group was 0.12 ± 0.22/mm^2, and the density of the TCMR group was 0.25 ± 0.34/mm^2 (P = 0.002). The density of infiltration NK cells was significantly higher in the ABMR group compared with the NR and the TCMR groups. (B) The density of infiltrated T cells in the ABMR group was 393.40 ± 300.93/mm^2, and the NP group was 129.83 ± 119.09/mm^2. The density of infiltrated T cells, CD3+CD56+ cells, was significantly higher in the ABMR group compared with the NR.

NR, no rejection; TCMR, T cell-mediated rejection; ABMR, antibody-mediated rejection. ∗P < 0.01

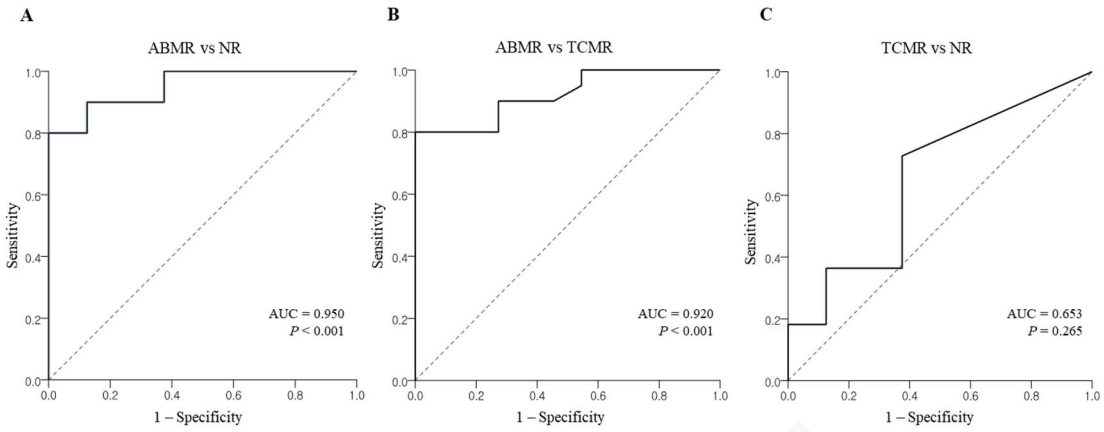

Figure 3. The association between the association between ABMR and the density of NK cell infiltration using logistic regression analysis.

AUC, area under the curve; NR, no rejection; TCMR, T cell-mediated rejection; ABMR, antibody-mediated rejection.

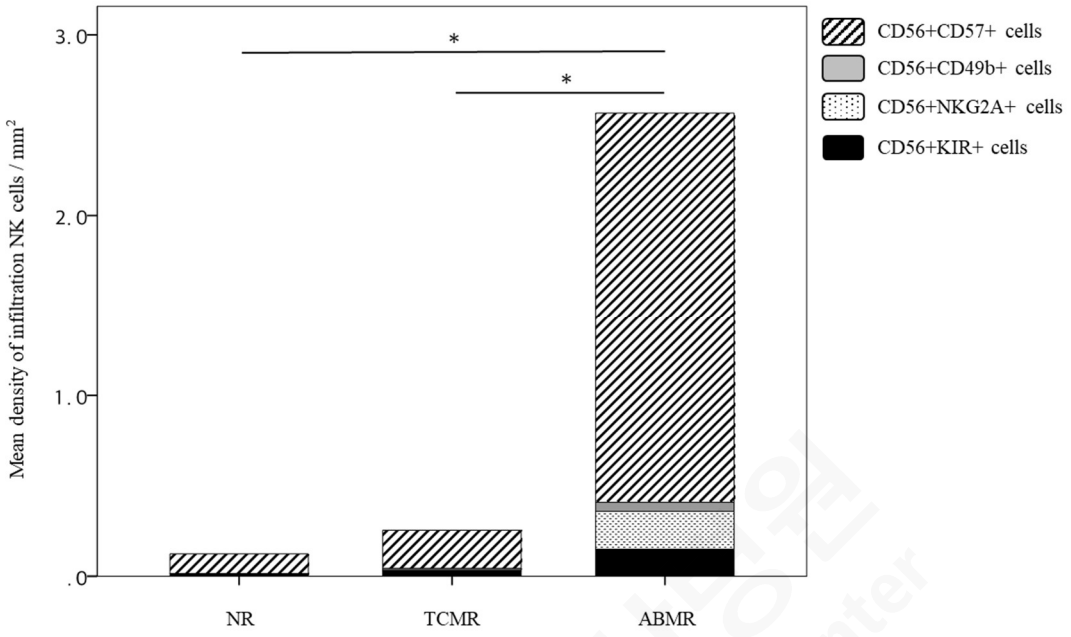

Figure 4. Mean density of infiltration NK cells according to histologic diagnosis.

CD56+CD57+ infiltrations were the most predominant subpopulation of infiltrated NK cells in the ABMR group.

NR, no rejection; TCMR, T cell-mediated rejection; ABMR, antibody-mediated rejection. ∗P < 0.05, a statistical significance in comparing the density of CD56+CD57+ cells between three groups

Infiltrated NK cells correlate with histological lesions and DSA

The correlation between the density of infiltrated NK cells and histological lesions scores was investigated. Pearson correlation was calculated; as a result, the density of infiltrated NK cells was significantly correlated with i (r = .423, P = .007), ti (r = .552, P < .001), ci (r = .425, P = .007), ct (r = .325, P = .044), and ptc (r = .489, P = .002) scores whereas g score (r = .309, P = .0.056) was associated with the density of infiltrated NK cells with marginal significance (Figure 5). It is likely that the mean fluorescence intensity (MFI) of DSA was correlated with the frequency of infiltrated NK cells (r = .317, P = .050) as well as infiltrated $CD56^{+}CD57^{+}$ cells (r = .294, P = 0.07), however, without a statistical significance.

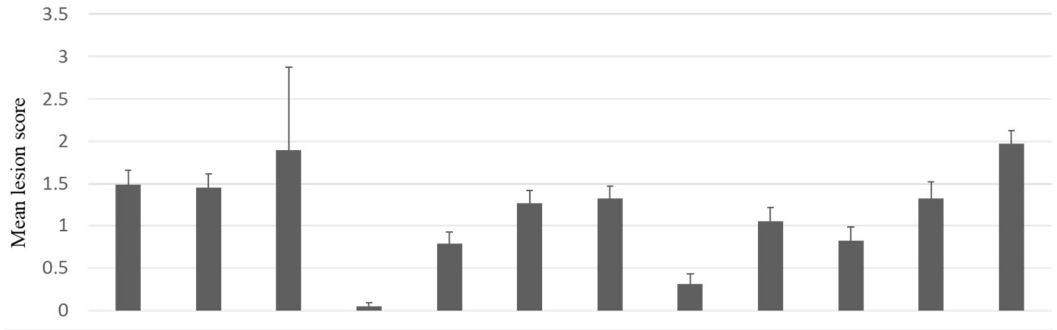

Density of intragraft NK cells	i	t	ti	v	g	ci	ct	cg	cv	ah	ptc	i-IFTA
	0.423*	0.171	0.552*	-0.119	0.309	0.425*	0.325*	0.184	-0.115	-0.058	0.489*	0.209
	Spearman's r											

Figure 5. Association between the density of infiltration NK cells and histologic lesions.

Mean lesion scores were calculated for each listed histologic lesion (i, interstitial inflammation; t, tubulitis; v, intimal arteritis; ptc, peritubular capillaritis; g, glomerulitis; cg, transplant glomerulopathy; ci, interstitial fibrosis; ct, tubular atrophy). Corresponding Spearman's correlation coefficients between the density of intragraft NK cells and the listed histologic lesion scores are shown. $*P < 0.05$

Effect of NK cell infiltration on kidney allograft failure

A univariable Cox regression analysis was used to evaluate the impact of baseline characteristics and histological factors on death-censored graft failure after indication biopsy, and the resultant significant factors were entered into a multivariable model (Table 3). Multivariable analysis revealed that presence of infiltrated NK cells (adjusted hazard ratio (AHR), 10.6; 95% confidence interval (CI), 1.01 – 110.82; P = .049), serum creatinine at the time of biopsy (AHR, 1.66; 95% CI, 1.12 – 2.45; P = .012), and diabetes (AHR, 11.68; 95% CI, 1.85 – 73.85; P = .009) were independently associated with death-censored graft failure after indication biopsy. Importantly, recipients with NK cell infiltrations had a significantly higher rate of death-censored graft failure compared with those without NK cell infiltrations (P = 0.025, Figure 6A). Although there was no significant difference in death-censored graft survival between the two groups, the death-censored graft survival in those with $CD56^{+}CD57^{+}$ NK cell infiltrations tends to be lower compared with those without those cells (Figure 6B).

Table 3. Death-censored graft failure and adjusted HR from multivariate Cox regression

Variables	HRunadj (95% CI)	HRadj (95% CI)	P-value
Presence of infiltrated NK cells	7.81 (0.97 – 63.18)	10.60 (1.01 – 110.82)	0.049
Serum creatinine at the time of biopsy, mg/dL	1.38 (1.03 – 1.86)	1.66 (1.12 – 2.45)	0.012
Chronic active ABMR	4.03 (1.13 – 14.32)	1.01 (0.21 – 4.83)	0.986
Diabetes	3.45 (0.97 – 12.3)	11.68 (1.85 – 73.85)	0.009

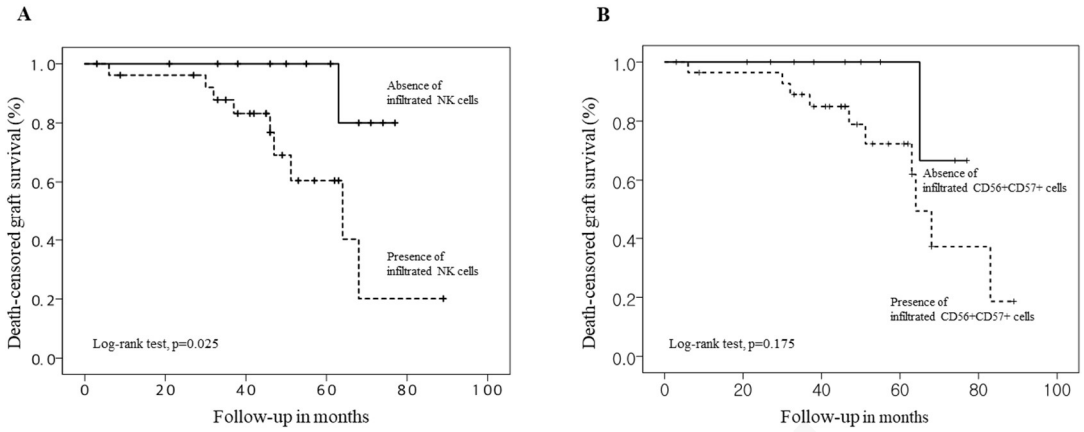

Figure 6. Kaplan-Meier curve for death-censored kidney allograft survival

Kaplan-Meier curve for 8-year death-censored kidney allograft survival according to the presence of infiltration NK cells (A) and the presence of CD56+CD57+ cells (B). Death-censored graft failure in recipients with infiltrated NK cells and infiltrated CD56+CD57+ cells in their for-cause biopsy was significantly higher compared with those without infiltrated NK cells and infiltrated CD56+CD57+ cells.

Discussion

In this study, the correlation between ABMR and the density of infiltrated NK cells in for-cause biopsies was demonstrated. Especially, $CD56^{+}CD57^{+}$ infiltrations, in kidney allograft, were the most predominant subset among the infiltrated NK cells. Furthermore, it was demonstrated that NK cell infiltration in kidney allografts was associated with poor death-censored graft survival. To our knowledge, this study is one of the few that used the multiplex immunohistochemistry technique to demonstrate an association between the high density of overall NK cell infiltration and ABMR. Notably, the specific subset of infiltrated NK cells ($CD3^{-}CD56^{+}CD57^{+}$), related to ABMR, was identified and confirmed in the multiplex immunohistochemistry.

The association between intrarenal NK cell transcripts with ABMR has been reported in the past. A different role of NK cells in the last ABMR was verified by *Hidalgo et al.* in addition to they proved a role for NK-transcript expressing cells in both TCMR and inflammation-associated injury and atrophy scarring[13,28]. Microarray analysis of kidney allograft with ABMR was used to demonstrate that NK cells are involved in ABMR through CD16a Fc receptors[12]. Likewise, *Yazdani et al.* proved that association between ABMR and an intrarenal expression signature enriched with NK cell pathways[11]; however, in contrast to other studies, activated NK cells were reported as only cell types to distinguish ABMR from TCMR, and the NK cells have predictive value for transplant outcomes. In their study, Yazdani et al. only used NKp46 as a single phenotypic marker to identify infiltrated NK cells and analyzed only nine cases of ABMR[11]. On the other hand, to better classify the specific subsets of infiltrated NK cells, we used seven-color multiplex immunohistochemistry to simultaneously analyze six markers fluorophores (KIR, CD3, CD56, NKG2A, CD57, and CD49b), in each FFPE tissue section from 20 cases of ABMR. The results were clearly observed that $CD3^{-}CD56^{+}CD57^{+}$ NK cells in the for-cause biopsy specimens were significantly associated with ABMR.

In this study, $CD56^{+}CD57^{+}$ NK cells were the major subpopulation in kidney allografts

of ABMR cases. The size of CD57 antigen is a 100 – 115 kD terminally sulfated carbohydrate epitope that was initially described as a marker of human natural killer cells. While CD57 expression on human lymphocytes reveals an inability to proliferate, these cells also display high cytotoxic potential while exhibiting both memory-like features and potent effector functions[29]. Remarkably, it has been reported that the expansion of CD57+ NK cells could be induced by viral infections such as human immunodeficiency virus and cytomegalovirus[30,31]. Moreover, hyper-responsive to CD16 ligation, which impersonates antibody-dependent cell-mediated cytotoxicity (ADCC), might be provided by the increased expression of CD16 through CD57+CD56dimCD16+ NK cells. Mature NK cells show substantial cytotoxic potential as suggested by high expression of the degranulation marker CD107a, granzyme B, and perforin[29]. It has been reported that NK cells are involved in ABMR by CD16a Fc receptors triggering ADCC[12]; however, it is not clearly demonstrated how CD57+ NK cells interact with CD16a to induce ADCC. Besides CD56+CD57+ NK cells, other subsets of infiltrated NK cells were predominant in the ABMR group even if the density of each subset was lower than CD56+CD57+ NK cells. As known as by previous reports, CD56+NKG2A+ and CD56+KIR+ NK cells inactivate NK cells interacting with HLA-E and distinct sets of classical HLA class I molecules[19-21]. The functional studies are necessary to determine whether CD56+NKG2A+ and CD56+KIR+ counteract the effects of CD56+CD57+ NK cells in further study. On the other hand, CD49b has been identified as one of conventional NK cell maturation-associated molecules[32-35]. The studies of $CD49a^{+}CD49b^{-}$ NK cells recently reported that $CD49a^{+}CD49b^{-}$ NK cells are tissue-resident in liver, uterus, and skin[36,37]. It has not been clarified whether CD56+CD49b+ NK cells have a distinction of characteristics contrast to CD56+CD49b- NK cells in a human kidney allograft.

In the observation of this study, TCMR group also had $CD56^{+}CD57^{+}$ NK cells in the kidney allografts, although the proportion of $CD56^{+}CD57^{+}$ NK cells was significantly lower than ABMR group. Considering that borderline rejection was predominant in the TCMR group and that about 27 percent of recipients in the TCMR group had DSA at the time of biopsy, it is possible that there was an antibody-mediated injury in the TCMR group without pathologic

evidence. On the other hand, this is in line with the results of a previous study, which demonstrated that CD16a-activated NK cells in ABMR and CD3/TCR-activated T cells in TCMR are highly similar in terms of rejection pathogenesis[38]. This study is limited in that because there were relatively few cases of ABMR available for analysis, and that a portion of the ABMR group had mixed phenotype of TCMR and ABMR. Nevertheless, the density of infiltration NK cells in the mixed rejection (TCMR+ABMR) cases was significantly higher compared with the TCMR group, thus justifying their inclusion in the ABMR group. Also, because of the small sample size of the study population and the single-center design of the study, the cut-off value for the density of NK cell infiltrations was not able to designate for discriminating among different clinical outcomes. In addition, infiltrated cells in five samples were positive for more than three out of four NK markers (CD57, CD49b, NKG2A, and KIR); therefore, for those samples, infiltration cells were counted repeatedly and divided by the number of positive markers to belong to each group in Figure 4. Nevertheless, densities of $CD56^{+}CD49b^{+}$, $CD56^{+}NKG2A^{+}$, and $CD56^{+}KIR^{+}$ were much lower compared with the $CD56^{+}CD57^{+}$ group. Initially, the clinical implications of each NK cell subset with respect to graft survival were intended to investigate. However, the relevant analysis was insufficient because of the low density of some NK subsets in addition to the small sample size of this study. In the hypothesis, it is important to understand the mechanisms of NK cell subsets and functional significances of co-expression of NK markers. For those purposes, however, it is necessary to confirm in vitro study with cell lines in a future study. Despite several limitations, this study is worthy in that it revealed the association between NK cell infiltration and poor clinical outcomes. Association between the higher numbers of CD56+ cell infiltration in for-cause biopsy and poor clinical outcomes was already reported in our previous study[27]. A prospective multi-center study should be carried out in order to evaluate the long-term clinical implications of NK cell infiltration observed in protocol biopsy as well as in for-cause biopsy. Finally, the exact mechanisms of influence of NK cells in ABMR or ADCC were not fully investigated. The results of the study suggest that CD57 is an important mediator between NK cells and ABMR. Therefore, comprehensive in vitro and in vivo studies are needed to define

the role of CD57 in NK cell-mediated graft injury. In this regard, a combination of technics, which have the possibilities for multiple comparison analyses, such as multiplex immunohistochemistry and microarray transcription analysis would be beneficial for more detailed characterization and analysis of infiltration NK cells.

Conclusion

In conclusion, we demonstrated that the presence of NK cells in the for-cause biopsy of kidney allografts was significantly associated with ABMR and poor graft survival. It is noteworthy that $CD56^{+}CD57^{+}$ infiltrates were the most predominant subset of infiltrated NK cells in renal transplant biopsies with ABMR. To determine the mechanism of NK cell infiltrations in kidney allografts of patients with ABMR is necessary for further studies.

References

1 Einecke, G. *et al.* Antibody-mediated microcirculation injury is the major cause of late kidney transplant failure. *Am J Transplant* **9**, 2520-2531, doi:10.1111/j.1600-6143.2009.02799.x (2009).

2 Sellares, J. *et al.* Understanding the causes of kidney transplant failure: the dominant role of antibody-mediated rejection and nonadherence. *Am J Transplant* **12**, 388-399, doi:10.1111/j.1600-6143.2011.03840.x (2012).

3 El-Zoghby, Z. M. *et al.* Identifying specific causes of kidney allograft loss. *Am J Transplant* **9**, 527-535, doi:10.1111/j.1600-6143.2008.02519.x (2009).

4 Naesens, M. *et al.* The histology of kidney transplant failure: a long-term follow-up study. *Transplantation* **98**, 427-435, doi:10.1097/TP.0000000000000183 (2014).

5 Pineiro, G. J. *et al.* Rituximab, plasma exchange and immunoglobulins: an ineffective treatment for chronic active antibody-mediated rejection. *BMC Nephrol* **19**, 261, doi:10.1186/s12882-018-1057-4 (2018).

6 Eskandary, F. *et al.* A Randomized Trial of Bortezomib in Late Antibody-Mediated Kidney Transplant Rejection. *J Am Soc Nephrol* **29**, 591-605, doi:10.1681/ASN.2017070818 (2018).

7 Sandal, S. & Zand, M. S. Rational clinical trial design for antibody mediated renal allograft injury. *Front Biosci (Landmark Ed)* **20**, 743-762 (2015).

8 Fildes, J. E. *et al.* Natural killer cells in peripheral blood and lung tissue are associated with chronic rejection after lung transplantation. *J Heart Lung Transplant* **27**, 203-207, doi:10.1016/j.healun.2007.11.571 (2008).

9 Kitchens, W. H. *et al.* The changing role of natural killer cells in solid organ rejection and tolerance. *Transplantation* **81**, 811-817, doi:10.1097/01.tp.0000202844.33794.0e (2006).

10 Meehan, A. C. *et al.* Natural killer cell activation in the lung allograft early posttransplantation. *Transplantation* **89**, 756-763, doi:10.1097/TP.0b013e3181cab17f (2010).

11 Yazdani, S. *et al.* Natural killer cell infiltration is discriminative for antibody-mediated rejection and predicts outcome after kidney transplantation. *Kidney Int* **95**, 188-198, doi:10.1016/j.kint.2018.08.027 (2019).

12 Venner, J. M., Hidalgo, L. G., Famulski, K. S., Chang, J. & Halloran, P. F. The Molecular Landscape of Antibody-Mediated Kidney Transplant Rejection: Evidence for NK Involvement Through CD16a Fc Receptors. *American Journal of Transplantation* **15**, 1336-1348, doi:10.1111/ajt.13115 (2015).

13 Hidalgo, L. G. *et al.* NK cell transcripts and NK cells in kidney biopsies from patients with donor-specific antibodies: evidence for NK cell involvement in antibody-mediated rejection. *Am J Transplant* **10**, 1812-1822, doi:10.1111/j.1600-6143.2010.03201.x (2010).

14 Sze, D. M. *et al.* Clonal cytotoxic T cells are expanded in myeloma and reside in the CD8(+)CD57(+)CD28(-) compartment. *Blood* **98**, 2817-2827, doi:10.1182/blood.v98.9.2817 (2001).

15 Lopez-Verges, S. *et al.* CD57 defines a functionally distinct population of mature NK cells in the human CD56dimCD16+ NK-cell subset. *Blood* **116**, 3865-3874, doi:10.1182/blood-2010-04-282301 (2010).

16 Krishnaraj, R. & Svanborg, A. Preferential accumulation of mature NK cells during human immunosenescence. *J Cell Biochem* **50**, 386-391, doi:10.1002/jcb.240500407 (1992).

17 Foley, B. *et al.* Cytomegalovirus reactivation after allogeneic transplantation promotes a lasting increase in educated NKG2C+ natural killer cells with potent function. *Blood* **119**, 2665-2674, doi:10.1182/blood-2011-10-386995 (2012).

18 Nielsen, C. M., White, M. J., Goodier, M. R. & Riley, E. M. Functional Significance of CD57 Expression on Human NK Cells and Relevance to Disease. *Front Immunol* **4**, 422, doi:10.3389/fimmu.2013.00422 (2013).

19 Lanier, L. L. Up on the tightrope: natural killer cell activation and inhibition. *Nat Immunol* **9**, 495-502, doi:10.1038/ni1581 (2008).

20 Moretta, A. *et al.* Activating receptors and coreceptors involved in human natural killer cell-mediated cytolysis. *Annu Rev Immunol* **19**, 197-223, doi:10.1146/annurev.immunol.19.1.197 (2001).

21 Crespo, M. *et al.* Circulating NK-cell subsets in renal allograft recipients with anti-HLA donor-specific antibodies. *Am J Transplant* **15**, 806-814, doi:10.1111/ajt.13010 (2015).

22 Go, H., Shin, S., Kim, Y. H., Han, D. J. & Cho, Y. M. Refinement of the criteria for ultrastructural peritubular capillary basement membrane multilayering in the diagnosis of chronic active/acute antibody-mediated rejection. *Transpl Int* **30**, 398-409, doi:10.1111/tri.12921 (2017).

23 Loupy, A. *et al.* The Banff 2015 Kidney Meeting Report: Current Challenges in Rejection Classification and Prospects for Adopting Molecular Pathology. *Am J Transplant* **17**, 28-41, doi:10.1111/ajt.14107 (2017).

24 Haas, M. *et al.* The Banff 2017 Kidney Meeting Report: Revised diagnostic criteria for chronic active T cell-mediated rejection, antibody-mediated rejection, and prospects for integrative endpoints for next-generation clinical trials. *Am J Transplant* **18**, 293-307, doi:10.1111/ajt.14625 (2018).

25 Park, I. J. *et al.* Prediction of radio-responsiveness with immune-profiling in patients with rectal cancer. *Oncotarget* **8**, 79793-79802, doi:10.18632/oncotarget.19558 (2017).

26 Carstens, J. L. *et al.* Spatial computation of intratumoral T cells correlates with survival of patients with pancreatic cancer. *Nat Commun* **8**, 15095, doi:10.1038/ncomms15095 (2017).

27 Shin, S. *et al.* Interpreting CD56+ and CD163+ infiltrates in early versus late renal transplant biopsies. *Am J Nephrol* **41**, 362-369, doi:10.1159/000430473 (2015).

28 Hidalgo, L. G. *et al.* Interpreting NK cell transcripts versus T cell transcripts in renal transplant biopsies. *Am J Transplant* **12**, 1180-1191, doi:10.1111/j.1600-6143.2011.03970.x (2012).

29 Kared, H., Martelli, S., Ng, T. P., Pender, S. L. & Larbi, A. CD57 in human natural killer cells and T-lymphocytes. *Cancer Immunol Immunother* **65**, 441-452, doi:10.1007/s00262-016-1803-z (2016).

30 Lugli, E., Marcenaro, E. & Mavilio, D. NK Cell Subset Redistribution during the Course of Viral Infections. *Front Immunol* **5**, 390, doi:10.3389/fimmu.2014.00390 (2014).

31 Makwana, N. *et al.* CMV drives the expansion of highly functional memory T cells expressing NK-cell receptors in renal transplant recipients. *Eur J Immunol* **47**, 1324-1334, doi:10.1002/eji.201747018 (2017).

32 Goh, W. & Huntington, N. D. Regulation of Murine Natural Killer Cell Development. *Front Immunol* **8**, 130, doi:10.3389/fimmu.2017.00130 (2017).

33 Kim, S. *et al.* In vivo developmental stages in murine natural killer cell maturation. *Nat Immunol* **3**, 523-528, doi:10.1038/ni796 (2002).

34 Huntington, N. D. *et al.* NK cell maturation and peripheral homeostasis is associated with KLRG1 up-regulation. *J Immunol* **178**, 4764-4770, doi:10.4049/jimmunol.178.8.4764 (2007).

35 Chiossone, L. *et al.* Maturation of mouse NK cells is a 4-stage developmental program. *Blood* **113**, 5488-5496, doi:10.1182/blood-2008-10-187179 (2009).

36 Peng, H. *et al.* Liver-resident NK cells confer adaptive immunity in skin-contact inflammation. *J Clin Invest* **123**, 1444-1456, doi:10.1172/JCI66381 (2013).

37 Sojka, D. K. *et al.* Tissue-resident natural killer (NK) cells are cell lineages distinct from thymic and conventional splenic NK cells. *Elife* **3**, e01659, doi:10.7554/eLife.01659 (2014).

38 Parkes, M. D., Halloran, P. F. & Hidalgo, L. G. Mechanistic Sharing Between NK Cells in ABMR and Effector T Cells in TCMR. *American Journal of Transplantation* **18**, 63-73, doi:10.1111/ajt.14410 (2018).

국문요약 (Korean Abstract)

신장이식 환자의 이식편내에 존재하는 자연살해세포 (natural killer cells)의 특정 서브 세트의 특성 및 임상적 영향에 대해서는 거의 알려져 있지 않다. 본 연구는 2017년 7월부터 2015년 5월까지 서울아산병원에서 수술을 시행한 환자 중 거부반응이 의심되는 환자 39명의 신장 생검조직을 분석하였다. 조직병리학적 보고서에 따라 거부반응이 없는 군(no rejection, NR) 8명, 세포매개성 거부반응만 가지고 있는 환자군(T cell mediated rejection only, TCMR) 11명, 항체매개성 거부반응군(antibody mediated rejection, ABMR) 20명으로 분류하였다. 본 연구 결과에서 NK 세포는 CD3-CD56+ 림프구(lymphocytes)이면서 한가지 이상의 NK 세포의 서브 세트인 CD57, CD49b, NKG2A, KIR과 함께 positive(양성)인 세포로 정의하였다. NK 세포의 밀도(density)는 항체매개성 거부반응 군(ABMR) (2.57 ± 2.58/mm^2)에서 거부반응이 없는 군(NR) (0.12 ± 0.22 /mm^2) 과 세포매개성 거부반응 군(TCMR) (0.25 ± 0.34/mm^2) 보다 유의하게 높은 결과를 보였다(P = .002). 특히, CD3-CD56+CD57+ 침윤세포 (2.16 ± 1.89)은 항체매개성 거부반응 군 (ABMR)에서 $CD56^+CD49b^+$ (0.05 ± 0.13), $CD56^+NKG2A^+$ (0.21 ± 0.69), $CD56^+KIR^+$ (0.15 ± 0.42) 세포와 비교하여 가장 빈번하게 관찰되었다(P < .001). 이식 실패 (Death-censored graft failure)는 자연살해세포 (NK cells)가 이식편에 침윤된 환자들이 침윤된 자연살해 세포(NK cells)가 없는 환자들 보다 유의하게 높은 수치를 보였다 (Log-rank test, P = .025). 본 연구의 결과를 종합하였을 때, 이식편에 침윤된 CD56+CD57+ 세포가 항체매개성 거부반응 (ABMR)을 가진 신장이식 환자의 자연살해 세포 (NK cells)의 주된 서브 세트이다. 그리고 침윤된 자연살해 세포 (NK cells)은 유의하게 이식 후 이식실패에 연관성이 있다.